

Negative refractive index induced by percolation in disordered metamaterials

Brian A. Slovick*

Applied Optics Laboratory, SRI International, Menlo Park, California 94025, United States

An effective medium model is developed for disordered metamaterials containing a spatially random distribution of dielectric spheres. Similar to effective medium models for ordered metamaterials, this model predicts resonances in the effective permeability and permittivity arising from electric- and magnetic-dipole Mie resonances in the spheres. In addition, the model predicts a redshift of the electric resonance with increasing particle loading. Interestingly, when the particle loading exceeds the percolation threshold of 33%, the model predicts that the electric resonance overlaps with the magnetic resonance, resulting in a negative refractive index.

Metamaterials, inhomogeneous composite materials that behave macroscopically as homogeneous materials, are of great fundamental and technological interest. The ability to tailor the macroscopic electromagnetic parameters, namely the permittivity and permeability, by changing the geometry and arrangement of the included elements has led to a number of important material designs and applications [1]. Most notable among these are materials with negative refractive index [2, 3], which have both negative permittivity and permeability. Negative index materials exhibit unusual properties such as negative refraction and exponential growth of evanescent near fields, which have been utilized for applications such as cloaking [4] and superresolution imaging [5].

To date, the metamaterial literature has focused primarily on designs where the included elements are arranged in a periodic lattice [6]. This is largely due to the ease of computation and suppression of scattering, as disorder of the lattice leads to spatial inhomogeneities. However, fabrication of periodic metamaterials on a large scale can be cost prohibitive, particularly for metamaterials operating in the optical band, where the lattice dimensions are submicron and require the use of electron-beam lithography [7, 8]. Self-assembly based nanosphere lithography has been used to fabricate centimeter-scale optical metasurfaces [9], but this approach is not scalable to much larger areas.

Disordered metamaterials provide a scalable alternative to periodic structures, provided that the scattering can be managed and their performance can be predicted. However, relatively few works have focused on disordered metamaterials. These limited studies have shown that size [10–12] and positional [13–19] disorder of a metamaterial’s resonator elements lead to resonance broadening and effective scattering loss. While these works provide important insights, they overlook one of the most important aspects of disorder: percolation. Percolation occurs in random composites at high loading when the particles form a continuous path through the composite, and it can have dramatic consequences on the effective electromagnetic parameters [20, 21]. For example, in metal-dielectric composites, percolation leads to a metal-insulator transition [20], which can be exploited

to obtain materials with ultrahigh dielectric constant for use as supercapacitors [21]. However, to date percolation studies have considered composites containing subwavelength or polydisperse particles, in which Mie scattering resonances are absent or dampened. An open question is how percolation impacts composites containing monodisperse, wavelength-sized particles that support collective Mie resonances.

In this Letter, it is shown that percolation induces a negative refractive index in disordered metamaterials containing Mie-resonant particles. To this end, the classic Bruggeman percolation theory [20, 22] is generalized to accommodate particle sizes comparable to the wavelength. Similar to effective medium models for ordered metamaterials [23–25], this model predicts resonances in the effective permeability and permittivity arising from electric- and magnetic-dipole Mie resonances in the spheres, as well as a redshift of the electric resonance as the loading of the particles increases. Interestingly, when the particle loading exceeds the percolation threshold of 33%, the electric resonance overlaps with the magnetic resonance, resulting in a negative refractive index. The possibility of obtaining a negative index in disordered metamaterials opens the door to more scalable designs suitable for practical large-area applications.

The model is derived by considering a composite medium containing a random dispersion of spherical particles in a matrix, which itself is represented as a space-filling random dispersion of infinitesimally small spheres. Similar to previous models [26, 27], the effective medium is defined such that the particles and matrix spheres, embedded in the effective medium, produce zero scattering and absorption (i.e., zero extinction). In this way, the effective medium is indistinguishable from the composite medium. Taking the extinction cross sections of the particle and matrix spheres to be σ_p and σ_m , respectively, the condition for zero extinction is

$$\sigma_p N_p + \sigma_m N_m = 0, \quad (1)$$

where N_p and N_m are the number densities of particles and matrix spheres, respectively. Since the particles and matrix spheres occupy the entire volume of the composite, the radius of the matrix spheres b must be chosen

such that

$$\frac{4}{3}\pi a^3 N_p + \frac{4}{3}\pi b^3 N_m = 1, \quad (2)$$

where a is the radius of the particles. The extinction cross sections can be calculated from the forward-scattering amplitude $S_j(0)$ using the optical theorem [26–28]

$$\sigma_j = \frac{4\pi}{k^2} \text{Re}[S_j(0)], \quad (3)$$

where $j = (m, p)$, $k = 2\pi/\lambda\sqrt{\epsilon\mu}$ is the wavenumber in the effective medium, where λ is the free-space wavelength, and ϵ and μ are the effective permittivity and permeability, respectively. The forward scattering amplitude, in turn, is related to electric and magnetic multipole Mie scattering coefficients, $a_{n,j}$ and $b_{n,j}$ by [28, 29]

$$S_j(0) = \frac{1}{2} \sum_{n=1}^{\infty} (2n+1)(a_{n,j} + b_{n,j}), \quad \text{where} \quad (4)$$

$$a_{n,j} = \frac{\sqrt{\epsilon_j/\epsilon} \psi'_n(ka) \psi_n(k_j a) - \sqrt{\mu_j/\mu} \psi_n(ka) \psi'_n(k_j a)}{\sqrt{\epsilon_j/\epsilon} \xi'_n(ka) \psi_n(k_j a) - \sqrt{\mu_j/\mu} \xi_n(ka) \psi'_n(k_j a)},$$

$$b_{n,j} = \frac{\sqrt{\mu_j/\mu} \psi'_n(ka) \psi_n(k_j a) - \sqrt{\epsilon_j/\epsilon} \psi_n(ka) \psi'_n(k_j a)}{\sqrt{\mu_j/\mu} \xi'_n(ka) \psi_n(k_j a) - \sqrt{\epsilon_j/\epsilon} \xi_n(ka) \psi'_n(k_j a)},$$

where ϵ_j and μ_j , respectively, are the permittivity and permeability of the particle or matrix, $k_j = 2\pi/\lambda\sqrt{\epsilon_j\mu_j}$, $\psi_n(x) = x j_n(x)$ and $\chi_n(x) = -x y_n(x)$ are the Riccati-Bessel functions where $j_n(x)$ and $y_n(x)$ are the spherical Bessel functions, $\xi_n(x) = \psi_n(x) - i\chi_n(x)$, and the primes denote differentiation with respect to the argument.

Substituting Eq. (3) into Eq. (1) and factorizing common terms, the condition for zero extinction reduces to

$$S_p(0)N_p + S_m(0)N_m = 0. \quad (5)$$

In order to obtain a closed-form solution to Eq. (5), several approximations are made. First, only the $n = 1$ dipolar terms in the expansion of $S_j(0)$ are considered. This approximation is valid as long as the spheres are subwavelength in size, as in the case of the matrix spheres, or have large refractive index relative to the background medium, as in the case of the particles. Second, the wavelength in the effective medium is assumed to be much larger than the particles (i.e., $ka \ll 1$). In this case, the Riccati-Bessel functions can be replaced by their small-argument approximations and the electric and magnetic dipole Mie scattering coefficients reduce to [23, 29]

$$a_{1,j} \approx -\frac{2i}{3}(ka)^3 \frac{\epsilon_j F(k_j a) - \epsilon}{\epsilon_j F(k_j a) + 2\epsilon}, \quad \text{and} \quad (6)$$

$$b_{1,j} \approx -\frac{2i}{3}(ka)^3 \frac{\mu_j F(k_j a) - \mu}{\mu_j F(k_j a) + 2\mu}, \quad \text{where} \quad (7)$$

$$F(x) = \frac{2\psi_1(x)}{x\psi_1'(x)} = \frac{2(\sin x - x \cos x)}{x \cos x + (x^2 - 1) \sin x}.$$

With these approximations, the condition for zero extinction in Eq. (5) reduces to

$$N_p a^3 \left[\frac{\epsilon_p F(k_p a) - \epsilon}{\epsilon_p F(k_p a) + 2\epsilon} + \frac{\mu_p F(k_p a) - \mu}{\mu_p F(k_p a) + 2\mu} \right] + N_m b^3 \left[\frac{\epsilon_m F(k_m b) - \epsilon}{\epsilon_m F(k_m b) + 2\epsilon} + \frac{\mu_m F(k_m b) - \mu}{\mu_m F(k_m b) + 2\mu} \right] = 0. \quad (8)$$

Similar to the original Bruggeman model [22], Eq. (8) is symmetric with respect to interchange of the particle and matrix. However, the focus of this work is on composites containing discrete, wavelength-sized particles dispersed in a continuous matrix, which can be represented as a space-filling dispersion of infinitesimally small particles. Thus, the matrix spheres are assumed to be much smaller than the wavelength, in which case $F(k_m b) = 1$.

Since the terms in Eq. (8) containing ϵ are independent of μ , and vice versa, the solution requires their sum to be zero. Noting that $N_p a^3$ is proportional to the volume fraction of particles f , and thus according to Eq. (2) $N_m b^3$ is proportional to $1 - f$, the solution to Eq. (8), assuming $F(k_m b) = 1$, is

$$f \frac{\epsilon_p F(k_p a) - \epsilon}{\epsilon_p F(k_p a) + 2\epsilon} + (1 - f) \frac{\epsilon_m - \epsilon}{\epsilon_m + 2\epsilon} = 0, \quad (9)$$

$$f \frac{\mu_p F(k_p a) - \mu}{\mu_p F(k_p a) + 2\mu} + (1 - f) \frac{\mu_m - \mu}{\mu_m + 2\mu} = 0. \quad (10)$$

Equations (9) and (10) are quadratic equations which can be solved to obtain the following closed-form expressions for the effective permittivity and permeability:

$$\epsilon = \frac{1}{4} \left\{ E \pm [E^2 + 8F(k_p a)\epsilon_p \epsilon_m]^{1/2} \right\}, \\ E = \epsilon_m(2 - 3f) + F(k_p a)\epsilon_p(3f - 1), \quad \text{and} \quad (11)$$

$$\mu = \frac{1}{4} \left\{ M \pm [M^2 + 8F(k_p a)\mu_p \mu_m]^{1/2} \right\}, \\ M = \mu_m(2 - 3f) + F(k_p a)\mu_p(3f - 1). \quad (12)$$

Several key properties of the model are now highlighted. First, to ensure thermodynamic passivity, the \pm signs must be chosen such that the imaginary parts of ϵ and μ are positive [25, 30]. Second, for particles much smaller than the wavelength, $F(k_p a) = 1$ and the model reduces to the classic Bruggeman mixing model [22, 26, 27]. Third, the effect of wavelength-sized particles, embodied in the resonant function $F(k_p a)$, is to multiply the effective permittivity and permeability of the particles. Near the Mie resonances, $F(k_p a)$ can be a large positive or negative number, leading to effectively large values of the particle permittivity and permeability, and thus resonances in ϵ and μ . Lastly, when ϵ_p or μ_p is large, or

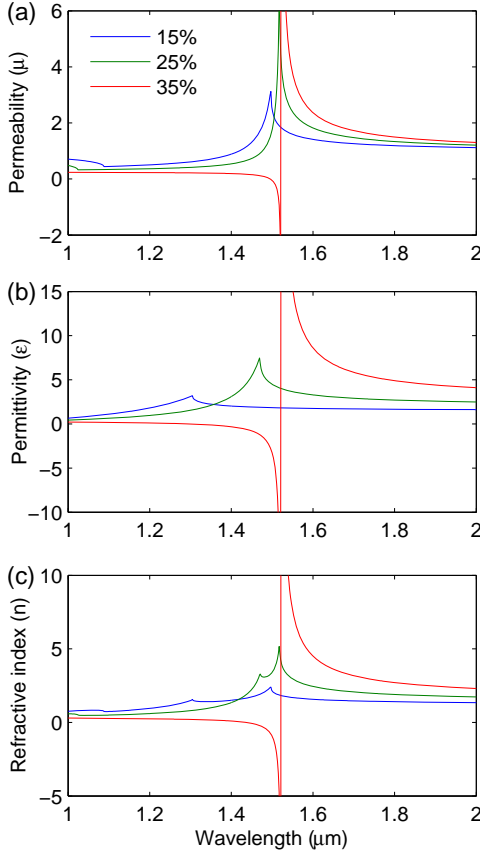


FIG. 1. Wavelength dependence of the real part of the effective permeability (a), permittivity (b), and refractive index (c) for 380 nm diameter Si spheres randomly dispersed in free space for different volume loading fractions.

the particle is resonant [i.e., $F(k_p a) \rightarrow \infty$], a percolation threshold occurs. This can be seen, for example, by taking the limit of Eq. (11) as $F(k_p a)\epsilon_p \rightarrow \infty$, in which case $\epsilon = 0$ for $f \leq 1/3$ and $\epsilon = \frac{1}{2}F(k_p a)\epsilon_p(3f-1)$ for $f > 1/3$. Since a similar argument applies to the effective permeability, beyond percolation both ϵ and μ are proportional to $F(k_p a)$, and thus their resonances, given by the poles of $F(k_p a)$, coincide to produce a negative index.

As an example of how percolation and Mie resonance induce a negative index, consider a metamaterial operating in the near infrared band consisting of 380 nm silicon (Si) spheres dispersed in free space. Silicon is chosen for its large refractive index, which is a requirement to obtain strong Mie resonances. The calculated wavelength dependence of the effective permeability, permittivity, and refractive index for different volume loading fractions, calculated using Eqs. (11) and (12), are shown in Fig. 1. For a relatively low loading of 15%, the magnetic-dipole Mie resonance gives rise to a resonance in the permeability at 1.5 μm, while the electric-dipole Mie resonance leads to a resonance in the effective permittivity at 1.3 μm. For this loading, the permeability and permittivity are both positive throughout the band. As the loading

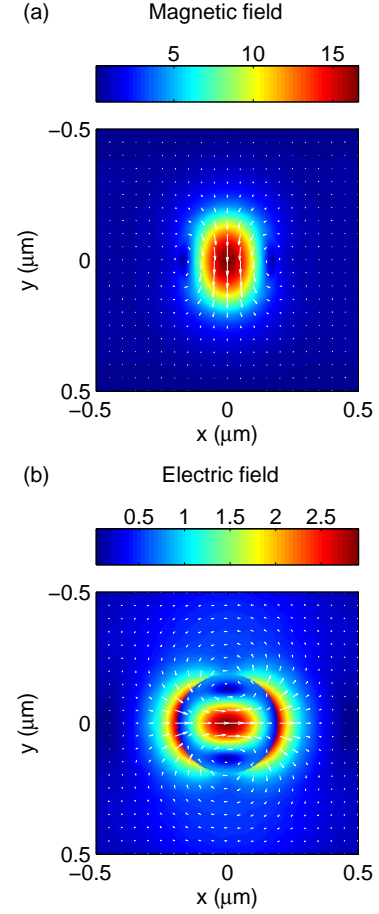


FIG. 2. Magnetic (a) and electric (b) fields at their respective Mie resonances for 380 nm diameter Si spheres in free space. The incident electric field is along x and propagation is into the page.

increases to 25%, the amplitude of both resonances increases, while the electric resonance in the permittivity shows a significant spectral redshift. Again, both parameters are positive for this loading. As the loading increases to 35%, which exceeds the percolation threshold of 33%, the redshift of the electric resonance causes it to overlap with the magnetic resonance. Since the permeability and permittivity are both negative near the resonance, the effective refractive index is also negative in the overlap region around 1.5 μm.

The reason why only the electric resonance undergoes a significant redshift can be understood from the electric and magnetic field distributions around the spheres at their respective resonances, shown in Fig. 2. While the magnetic field is well confined at the magnetic resonance (1.4 μm), the electric field at resonance (1.04 μm) shows considerable enhancement outside the sphere. The different degrees of confinement of the electric and magnetic fields can be traced to their different boundary conditions. Since the normal components of \mathbf{B} ($=\mu\mathbf{H}$) and \mathbf{D} ($=\epsilon\mathbf{E}$) must be continuous across the sphere surface,

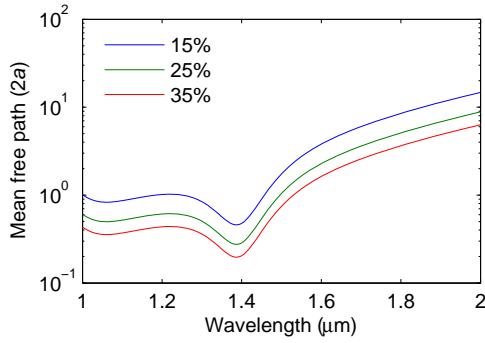


FIG. 3. Wavelength dependence of the mean free path for 380 nm diameter Si spheres randomly dispersed in free space for different volume loading fractions.

the normal component of \mathbf{H} is also continuous because $\mu = 1$ throughout, whereas the normal component of \mathbf{E} is discontinuous owing to the large dielectric mismatch between Si and free space. This leads to a larger normal component of \mathbf{E} just outside the sphere surface, and hence poor confinement. Alternatively, the normal component of \mathbf{H} is continuous, leading to better field confinement. The poor confinement of the electric field leads to interparticle coupling at high loading, lowering the energy of the electric dipole-dipole interaction, and red-shifting the resonance.

A drawback of disordered metamaterials is that their lack of periodicity leads to scattering loss, which limits the thickness of useful material to approximately one mean free path. Figure 3 shows the calculated mean free path, normalized to the particle diameter, for the material in Fig. 1. As expected, the mean free path decreases at shorter wavelengths, reaching a local minimum near the magnetic Mie resonance at $1.4 \mu\text{m}$. For 35% loading, the mean free path in the negative index region around $1.5 \mu\text{m}$ is approximately equal to the particle diameter. Thus, to obtain acceptable transmission in the disordered material with negative index, the thickness should be limited to approximately one unit cell.

In summary, the classic Bruggeman percolation model for disordered composites was generalized to support particle sizes comparable to the wavelength. Similar to effective medium models for ordered metamaterials, this model predicts that electric and magnetic Mie resonances in the spheres give rise to resonances in the effective permittivity and permeability of the composite. The model also predicts a redshift of the electric resonance with increasing particle loading due to particle interactions arising from poor confinement of the electric field. Most importantly, when the particle loading exceeds the percolation threshold of 33%, the electric resonance coincides with the magnetic resonance, resulting in a negative refractive index. The possibility of obtaining a negative index in disordered materials opens the door to more scalable designs suitable for large-area applications.

* Corresponding author: brian.slovick@sri.com

- [1] N. Engheta and R. W. Ziolkowski, *Metamaterials: physics and engineering explorations* (John Wiley & Sons, 2006).
- [2] D. R. Smith, W. J. Padilla, D. C. Vier, S. C. Nemat-Nasser, and S. Schultz, *Phys. Rev. Lett.* **84**, 4184 (2000).
- [3] V. M. Shalaev, *Nature Photon.* **1**, 41 (2007).
- [4] D. Schurig, J. J. Mock, B. J. Justice, S. A. Cummer, J. B. Pendry, A. F. Starr, and D. R. Smith, *Science* **314**, 977 (2006).
- [5] J. B. Pendry, *Phys. Rev. Lett.* **85**, 3966 (2000).
- [6] D. R. Smith, D. C. Vier, T. Koschny, and C. M. Soukoulis, *Phys. Rev. E* **71**, 036617 (2005).
- [7] A. Boltasseva and V. M. Shalaev, *Metamat.* **2**, 1 (2008).
- [8] D. B. Burckel, J. R. Wendt, G. A. T. Eyck, A. R. Ellis, I. Brener, and M. B. Sinclair, *Adv. Mat.* **22**, 3171 (2010).
- [9] P. Moitra, B. A. Slovick, W. Li, I. I. Kravchenko, D. P. Briggs, S. Krishnamurthy, and J. Valentine, *ACS Photon.* **2**, 692 (2015).
- [10] A. A. Zharov, I. V. Shadrivov, and Y. S. Kivshar, *J. Appl. Phys.* **97**, 113906 (2005).
- [11] M. V. Gorkunov, S. A. Gredeskul, I. V. Shadrivov, and Y. S. Kivshar, *Phys. Rev. E* **73**, 056605 (2006).
- [12] J. H. Gollub, T. Hand, S. Sajuyigbe, S. Mendonca, S. Cummer, and D. R. Smith, *Appl. Phys. Lett.* **91**, 162907 (2007).
- [13] K. Aydin, K. Guven, N. Katsarakis, C. Soukoulis, and E. Ozbay, *Opt. Express* **12**, 5896 (2004).
- [14] C. Helgert, C. Rockstuhl, C. Etrich, C. Menzel, E.-B. Kley, A. Tunnermann, F. Lederer, and T. Pertsch, *Phys. Rev. B* **79**, 233107 (2009).
- [15] N. Papasimakis, V. A. Fedotov, Y. H. Fu, D. P. Tsai, and N. I. Zheludev, *Phys. Rev. B* **80**, 041102 (2009).
- [16] R. Singh, X. Lu, J. Gu, Z. Tian, and W. Zhang, *J. Opt.* **12**, 015101 (2009).
- [17] J. M. Rico-García, J. M. López-Alonso, and A. Aradian, *JOSA B* **29**, 53 (2012).
- [18] S. Savo, N. Papasimakis, and N. I. Zheludev, *Phys. Rev. B* **85**, 121104 (2012).
- [19] P. Moitra, B. A. Slovick, Z. G. Yu, S. Krishnamurthy, and J. Valentine, *Appl. Phys. Lett.* **104**, 171102 (2014).
- [20] S. Kirkpatrick, *Rev. Mod. Phys.* **45**, 574 (1973).
- [21] C. Pecharrmán and J. S. Moya, *Adv. Mater.* **12**, 294 (2000).
- [22] D. A. G. Bruggeman, *Ann. Phys.* **24**, 636 (1935).
- [23] L. Lewin, *Elec. Eng. Part III: Rad. Comm. Eng., J. Inst. of* **94**, 65 (1947).
- [24] Y. Wu, J. Li, Z.-Q. Zhang, and C. T. Chan, *Phys. Rev. B* **74**, 085111 (2006).
- [25] B. A. Slovick, Z. G. Yu, and S. Krishnamurthy, *Phys. Rev. B* **89**, 155118 (2014).
- [26] D. Stroud and F. P. Pan, *Phys. Rev. B* **17**, 1602 (1978).
- [27] G. A. Niklasson, C. G. Granqvist, and O. Hunderi, *Appl. Optics* **20**, 26 (1981).
- [28] C. F. Bohren and D. R. Huffman, *Absorption and Scattering of Light by Small Particles* (Wiley, 1983).
- [29] E. F. Kuester, N. Memic, S. Shen, A. Scher, S. Kim, K. Kumley, and H. Loui, *Prog. Electromagn. Res.* **33**, 175 (2011).
- [30] L. D. Landau and E. M. Lifshitz, *Electrodynamics of Continuous Media* (Butterworth-Heinemann, 1984).